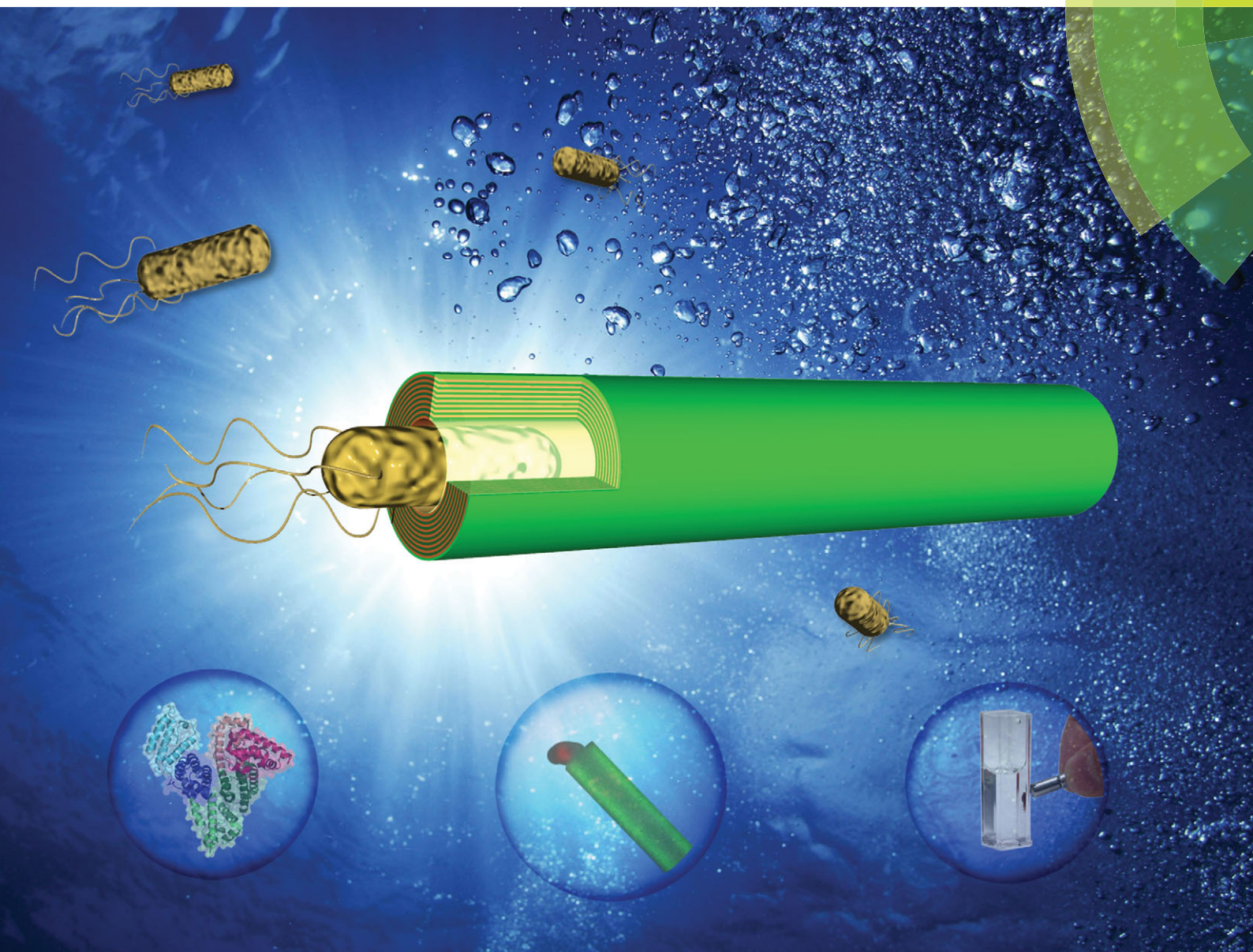


ChemComm

Chemical Communications

www.rsc.org/chemcomm



ISSN 1359-7345



COMMUNICATION

T. Komatsu *et al.*

An *Escherichia coli* trap in human serum albumin microtubes

An *Escherichia coli* trap in human serum albumin microtubes†

S. Yuge, M. Akiyama and T. Komatsu*

Cite this: *Chem. Commun.*, 2014, 50, 9640Received 14th May 2014,
Accepted 10th June 2014

DOI: 10.1039/c4cc03632h

www.rsc.org/chemcomm

We describe the template synthesis of human serum albumin microtubes (MTs) and highlight their *Escherichia coli* (*E. coli*) trapping capability with extremely high efficiency. The *E. coli* was loaded into the one-dimensional pore space interior of the tubule. Similar MTs including an Fe₃O₄ layer also captured *E. coli* and were manipulated by exposure to a magnetic field.

Hollow, cylindrical, nanometer-scale structures comprising biomaterials, *i.e.* bionanotubes, have attracted considerable attention because of their potential applications as molecular trapping devices, drug delivery containers, and enzymatic reactors.^{1–13} Alternate layer-by-layer (LbL) build-up assembly of proteins,^{4,6,7,9,10} DNAs,^{5,8,11} and antibodies^{12,13} in nanoporous membranes enables creation of structurally defined smart nanotubes (NTs) with versatile biochemical reactivities. The one-dimensional (1D) pore space interior of the tubule can be tailored by deposition of a desired material. Therefore, many investigators have explored the loading of nanometer-size entities into the channel, such as pharmaceutical drugs,^{9,12} bioactive spheres,⁹ inorganic colloids,¹¹ and infectious viruses.¹³ Another challenging subject in this field would be the trapping of a living organism. *Escherichia coli* (*E. coli*), a rod-shaped gram-negative bacterium, is the smallest organism of the micrometer-scale world (0.4–0.7 μm width, 2–4 μm length). Many strains are harmless, but some serotypes can cause severe poisoning in humans, such as enterohemorrhagic *E. coli* O157.¹⁴ If one were able to generate a unique *E. coli* trap in protein microtubes (MTs), then it would have an important contribution not only to bioseparation chemistry, but also to diverse aspects of human health. This communication is the first to describe the synthesis and structure of human serum albumin (HSA)-based MTs, and to highlight their excellent *E. coli* trapping capability.

The MTs were fabricated by template synthesis using electrostatic LbL assembly.⁹ Briefly, positively charged poly-L-arginine (PLA) and negatively charged HSA were alternately deposited (nine-cycles) onto the pore wall of a track-etched polycarbonate (PC) membrane (1.2 μm pore size). Subsequent dissolution of the PC framework in *N,N*-dimethylformamide and freeze-drying of the liberated core yielded (PLA/HSA)₉ MTs as white powder. SEM measurements revealed the formation of uniform hollow cylinders with 1.0 ± 0.02 μm outer diameter and 148 ± 5 nm wall thickness (Fig. 1a and b). The tube lengths (*ca.* 25 μm) coincided well with the PC membrane pore depth. In contrast, 12-layered (PLA/HSA)₁₂ MTs were wrinkled and fragile, which implies that six-cycle injection is insufficient to generate stiff MTs. We concluded that at least nine-cycle deposition is necessary to construct a robust 1 μm -width cylinder by our template synthesis. Based on the general principle of LbL membrane growth, we hypothesized a nine-layered cylinder model. The average thickness of a PLA/HSA bilayer in the MT is estimated to be 16.4 nm. If one postulates the dimensions of HSA to be 8 nm from the data of the single-crystal structure¹⁵ and small-angle X-ray scattering analyses,¹⁶ then the PLA layer thickness is calculated to be 8.4 nm, which is between the reported values for typical polyelectrolyte layers prepared in the porous template by a wet process.^{17–19}

The obtained (PLA/HSA)₉ MTs were dispersed in deionized water, yielding a slightly turbid solution. To evaluate the morphology and stability of the MTs in water, the aqueous dispersion was freeze-dried *in vacuo*. SEM images demonstrated that the tubular walls swelled considerably and that their thickness became 250 ± 7 nm in water (Fig. 1c). It is interesting that the outer diameter was unaltered (1.0 ± 0.04 μm). Consequently, the inner pore size diminished to *ca.* 500 nm. The average thickness of an individual PLA/HSA bilayer was measured to be 28 nm in water. Under the assumption that the HSA size did not change (≤ 8 nm),^{15,16} the PLA layer thickness might be 20 nm. This value is apparently larger than that of the dry form, but it is similar to the values of the polyelectrolyte layers in the NTs prepared under pressure conditions.^{9,20} We determined the swelling ratio of the PLA layer (α_{PLA} : a ratio between the section area in the swollen state

Department of Applied Chemistry, Faculty of Science and Engineering,
Chuo University, 1-13-27 Kasuga, Bunkyo-ku, Tokyo 112-8551, Japan.

E-mail: komatsu@kc.chuo-u.ac.jp

† Electronic supplementary information (ESI) available: Experimental section, the SEM image of *E. coli*, the CLSM image of CTC-*E. coli*, and the relationship between mixing time and cell viability of *E. coli*. See DOI: 10.1039/c4cc03632h



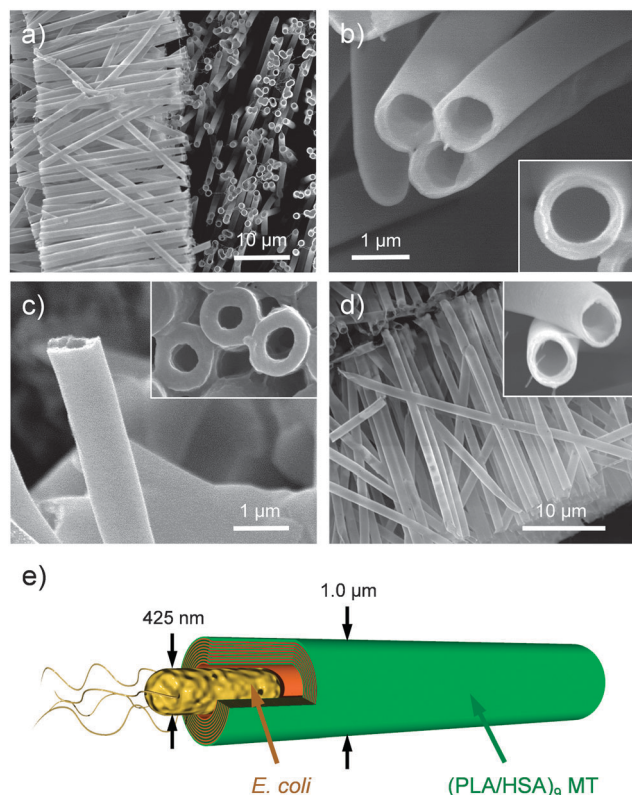


Fig. 1 SEM images of (PLA/HSA)₉ MTs prepared using a porous PC template ($D_p = 1.2 \mu\text{m}$): (a, b) dried samples and (c) lyophilized sample after swelling in water. (d) SEM image of Fe₃O₄(PLA/HSA)₉ MTs prepared using a porous PC template ($D_p = 1.2 \mu\text{m}$). (e) Schematic illustration of *E. coli* entrapped (PLA/HSA)₉ MTs.

and that in a dried state) to be 2.1 (see ESI[†]), which is almost identical to the data reported in the literature for general polyelectrolytes (1.2–4.0).^{21,22} Morphologies of the (PLA/HSA)₉ MTs were retained for more than 24 h in water at 25 °C.

Then we measured the *E. coli* capture capability of the (PLA/HSA)₉ MT. The dimensions of *E. coli* K12 (XL10-gold) we used were 425 nm width and approximately 2–3 μm length, as revealed by SEM measurements (Fig. S1, ESI[†]). The colony incidence of the sample solution after mixing with the MTs was assayed using a standard plate count method. First, *E. coli* ($1 \times 10^8 \text{ CFU mL}^{-1}$, 100 μL) was added to the aqueous solution of (PLA/HSA)₉ MTs (ca. 150 $\mu\text{g mL}^{-1}$, 900 μL).²³ The resultant mixture was incubated with gentle rotation at 25 °C for 1–30 min. Then a part of the solution was spread on the LB agar plate and cultured at 37 °C for 16 h. The colonies appearing on the plate [$N_c(\text{MT})$] were markedly fewer than those of identically treated *E. coli* without the tubes [$N_c(\text{control})$]. To our surprise, $N_c(\text{MT})$ became completely zero by 30 min mixing with the MTs (Fig. 2a and b); the disappearance yield ($100 - \text{colony incidence}$) reached 100%. Incubation with the 6-layered thin (PLA/HSA)₃ nanotubes (NTs) (ca. 200 nm inner diameter) exhibited no change in the colony number. We reasoned that the *E. coli* (425 nm width) entered the pore of the MT (ca. 500 nm), although it is too large to enter the narrow NT's channel (ca. 200 nm).

The incorporation of *E. coli* into the MT was proved using confocal laser scanning microscopy (CLSM). To visualize the tube,

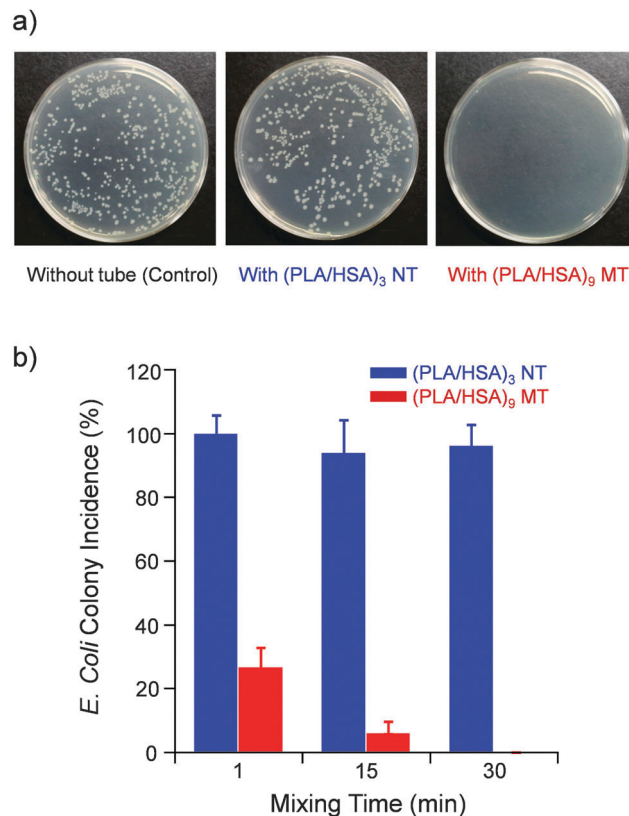


Fig. 2 (a) Appearance of LB agar plates spread with *E. coli* dispersion which was incubated with (PLA/HSA)₃ NTs or (PLA/HSA)₉ MTs for 30 min (after 16 h cell culture at 37 °C). (b) Relationship between mixing time and colony incidence [$N_c(\text{NT})$ or $N_c(\text{MT})/N_c(\text{control}) \times 100$] ($n = 3$).

a fluorescein-labeled HSA (f-HSA) was exploited as an intermediate layer component, yielding (PLA/HSA)₇PLA/f-HSA/PLA/HSA MTs (fluorescent MTs). *E. coli* was also stained with 5-cyano-2,3-ditolyl tetrazolium chloride (CTC). This labeling agent specifically stained the edge of the *E. coli* rod (Fig. S2, ESI[†]), which is quite helpful to distinguish the *E. coli* position in the tube. In CLSM images of the mixture solution, the tube wall fluoresced green (Em. 522 nm); the hollow structure was clearly visible. CTC-*E. coli* also showed sharp fluorescence in red (Em. 630 nm). Overlapping these pictures with a DIC image demonstrates that CTC-*E. coli* was loaded into the 1D pore space of the MT (Fig. 3). Remarkably, the edge of *E. coli* appeared from the mouse of the

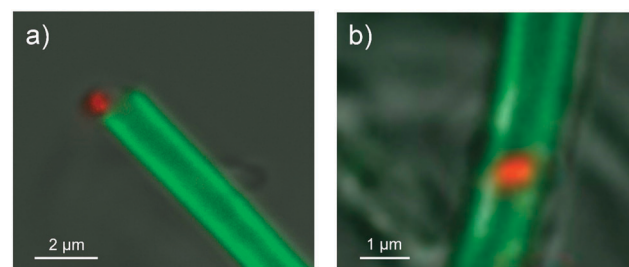


Fig. 3 Overlapping images of DIC and CLSM of fluorescent MTs incorporating CTC-*E. coli*. (a) CTC-*E. coli* remained at the terminal of the tube and (b) small CTC-*E. coli* reached the depth of the tube. Ex. 488 nm.



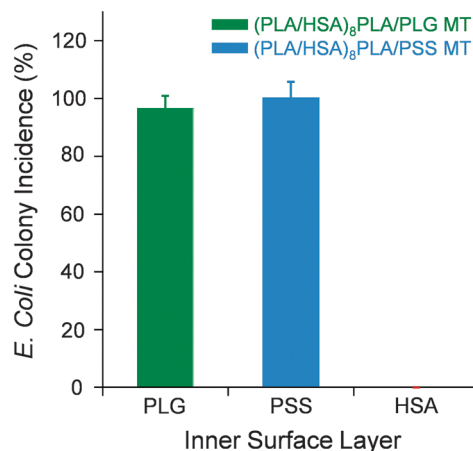


Fig. 4 Relationship between mixing time and colony incidence of *E. coli* ($n = 3$).

tube in most cases, thereby forming “bacterium-corked MT” (Fig. 1e and 3a). The *E. coli* width is only slightly smaller than the pore size (*ca.* 500 nm). Therefore it cannot enter deep inside of the tubule. Sometimes, a few *E. coli* are able to diffuse into the channel and reach the tube depth (Fig. 3b).

Does *E. coli* really like the 1D hollow microspace with high density of HSA? To make this point clear, we prepared comparable MTs with different interior surfaces using poly-L-glutamic acid sodium salt (PLG) and poly(sodium 4-styrenesulfonate) (PSS) (both negatively charged polymers) instead of the last layer of HSA. SEM measurements revealed that the (PLA/HSA)₈PLA/PLG MTs and (PLA/HSA)₈PLA/PSS MTs possess the same structures (outer/inner diameters and length) as (PLA/HSA)₉ MTs. Predictably, these MTs without the HSA pore wall could not capture *E. coli* (Fig. 4). We inferred that the inner surface wall of the tube must be comprised of HSA to entrap *E. coli*. HSA can reversibly bind many bacterial species by interacting with expressed surface proteins.²⁴ Bacteria move in response to a chemical stimulus, *i.e.* chemotaxis. For instance, *E. coli* directs its movements according to certain chemicals in the environment.²⁵ We reasoned that multiple factors contribute to the *E. coli* capture into the (PLA/HSA)₉ MT.

To clarify the fate of the entrapped *E. coli*, the cell viability was measured using WST assay. It is noteworthy that *E. coli* accommodated in the (PLA/HSA)₉ MT was metabolically inactive. After 1 h mixing, almost all *E. coli* lost cell proliferation ability (Fig. S3, ESI†). One possible explanation is that *E. coli* growth might be blocked by stopping cell deviation. In the narrow space of the MT, bacteria cannot reproduce through asexual reproduction by binary fission. Another proposed mechanism is degradation of the HSA wall by OmpT, which is an aspartyl protease found on the outer membrane of *E. coli*.²⁶ This protease on the *E. coli*'s surface comes into contact with the HSA inner-wall and cleaves the polypeptide. Subsequently, the exposed cationic PLA layer might cause cytotoxicity.

Moreover, we introduced a magnetite (Fe₃O₄) nanoparticle layer into the MT. Magnetic-field assisted bioseparation using spherical particles including Fe₃O₄ has been an area of particular recent interest because of its diverse medical applications.^{27,28}

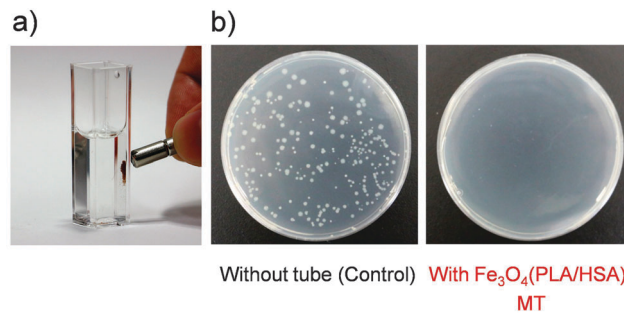


Fig. 5 (a) Photograph of collection of *E. coli*-loaded Fe₃O₄(PLA/HSA)₉ MTs by a magnetic field. (b) Appearance of LB agar plates spread with *E. coli* dispersion which was incubated with Fe₃O₄(PLA/HSA)₉ MTs for 30 min (after 16 h cell culture at 37 °C).

Nevertheless, few reports describe the use of hollow magnetic cylinders for bioseparation.^{12,17,29} An HSA-based MT bearing a ferrimagnetic layer would become a magnetically responsive trap for *E. coli*. The magnetic tubes were prepared using a similar LbL assembly procedure with Fe₃O₄ nanoparticles. SEM observations of the Fe₃O₄(PLA/HSA)₉ MTs revealed the formation of highly ordered arrays of the MTs with an outer diameter of $1.0 \pm 0.03 \mu\text{m}$ and the maximum length of *ca.* 25 μm (Fig. 1d). The wall thickness was $155 \pm 7 \text{ nm}$, which is slightly thicker than that observed in the (PLA/HSA)₉ MTs.

Finally, the *E. coli* capture ability of these magnetic MTs was evaluated. As expected, the Fe₃O₄(PLA/HSA)₉ MTs can be collected by exposure to a magnetic field. By bringing a neodymium magnet close to the quartz cuvette including the *E. coli* solution with the Fe₃O₄(PLA/HSA)₉ MTs, the brown tubes were attracted rapidly to the magnet; the solution became colourless (Fig. 5a). Detaching the magnet from the cuvette liberated the MTs in the aqueous phase. This magnetic-field-induced collection-dispersion was observed to be reversible. Then a part of the upper clear solution in a cuvette, in which the *E. coli* loaded-Fe₃O₄(PLA/HSA)₉ MTs were gathered at the bottom by the magnetic field, was spread on an LB agar plate and cultured at 37 °C for 16 h. The number of colonies appearing on the plate became zero after 30 min mixing with Fe₃O₄(PLA/HSA)₉ MTs (Fig. 5b). The disappearance yield reached 100%. We concluded that the *E. coli* entered the channel of Fe₃O₄(PLA/HSA)₉ MTs in a similar fashion to that of (PLA/HSA)₉ MTs.

In conclusion, the blood serum protein HSA microtubes ensnared the *E. coli* perfectly. The efficiency of removal by a single treatment with (PLA/HSA)₉ MTs was over $-7 \log$ order. This remarkable result will serve as a trigger to produce a new and productive field of removing device systems for bacteria. For example, elimination of enterohemorrhagic *E. coli* O157, using (PLA/HSA)₉ MTs, is expected to be of incredible medical importance. Furthermore, *E. coli*-loaded MTs containing an Fe₃O₄ layer were magnetically manipulated in solution. Recombinant HSA is currently manufactured on an industrial scale,³⁰ which enables production of these protein MTs for practical use.

This work was supported by a Grant-in-Aid for Scientific Research on Innovative Area “Coordination Programming” (Area 2107, No. 21108013) from MEXT Japan, Grant-in-Aid for



Challenging Exploratory Research (No. 26600030) from JSPS, and a Joint Research Grant from the Institute of Science and Engineering, Chuo University.

Notes and references

- 1 T. Shimizu, M. Masuda and H. Minamikawa, *Chem. Rev.*, 2005, **105**, 1401.
- 2 Y. Geng, P. Dalhaimer, S. Cai, R. Tsai, M. Tewari, T. Minko and D. E. Discher, *Nat. Nanotechnol.*, 2007, **2**, 249.
- 3 C. Valéry, F. Artzner and M. Paternostre, *Soft Matter*, 2011, **7**, 9583.
- 4 S. Hou, J. Wang and C. R. Martin, *Nano Lett.*, 2005, **5**, 231.
- 5 S. Hou, J. Wang and C. R. Martin, *J. Am. Chem. Soc.*, 2005, **127**, 8586.
- 6 A. Yu, Z. Liang and F. Caruso, *Chem. Mater.*, 2005, **17**, 171.
- 7 Y. Tian, Q. He, Y. Cui and J. Li, *Biomacromolecules*, 2006, **7**, 2539.
- 8 J. Jang, S. Ko and Y. Kim, *Adv. Funct. Mater.*, 2006, **16**, 754.
- 9 X. Qu and T. Komatsu, *ACS Nano*, 2010, **4**, 563.
- 10 T. Komatsu, *Nanoscale*, 2012, **4**, 1910.
- 11 C. J. Roy, N. Chorine, B. G. De Geest, S. De Smedt, A. M. Jonas and S. Demoustier-Champagne, *Chem. Mater.*, 2012, **24**, 1562.
- 12 S. J. Son, J. Reichel, B. He, M. Schuchman and S. B. Lee, *J. Am. Chem. Soc.*, 2005, **127**, 7316.
- 13 T. Komatsu, X. Qu, H. Ihara, M. Fujihara, H. Azuma and H. Ikeda, *J. Am. Chem. Soc.*, 2011, **133**, 3246.
- 14 H. Karch, P. I. Tarr and M. Bielaszewska, *Int. J. Med. Microbiol.*, 2005, **295**, 405.
- 15 A. A. Bhattacharya, T. Grüne and S. Curry, *J. Mol. Biol.*, 2000, **303**, 721.
- 16 T. Sato, T. Komatsu, A. Nakagawa and E. Tsuchida, *Phys. Rev. Lett.*, 2007, **98**, 208101.
- 17 D. Lee, R. E. Cohen and M. F. Rubner, *Langmuir*, 2007, **23**, 123.
- 18 S. Ai, G. Lu, Q. He and J. Li, *J. Am. Chem. Soc.*, 2003, **125**, 11140.
- 19 D. Lee, A. J. Nolte, A. L. Kunz, M. F. Rubner and R. E. Cohen, *J. Am. Chem. Soc.*, 2006, **128**, 8521.
- 20 H. Alem, F. Blondeau, K. Glinel, S. Demoustier-Champagne and A. M. Jones, *Macromolecules*, 2007, **40**, 3366.
- 21 S. T. Dubas and J. B. Schlenoff, *Langmuir*, 2001, **17**, 7725.
- 22 M. D. Miller and M. L. Bruening, *Chem. Mater.*, 2005, **17**, 5375.
- 23 To avoid an electrostatic or nonspecific attraction between the *E. coli* and (PLA/HSA)₉ MT's exterior surface, free HSA was added to the tube dispersion in advance ([HSA] = 0.2 mM).
- 24 S. Lejon, I.-M. Frick, L. Björck, M. Wikström and S. Svensson, *J. Biol. Chem.*, 2004, **279**, 42924.
- 25 V. Sourjik, *Trends Microbiol.*, 2004, **12**, 569.
- 26 L. Vandeputte-Rutten, R. A. Kramer, J. Kroon, N. Dekker, M. R. Egmond and P. Gros, *EMBO J.*, 2001, **20**, 5033.
- 27 A. Ito, M. Shinkai, H. Honda and T. Kobayashi, *J. Biosci. Bioeng.*, 2005, **100**, 1.
- 28 A. H. Latham and M. E. Williams, *Acc. Chem. Res.*, 2008, **41**, 411.
- 29 Q. He, Y. Tian, Y. Cui, H. Möhwald and J. Li, *J. Mater. Chem.*, 2008, **18**, 748.
- 30 K. Kobayashi, *Biologicals*, 2006, **34**, 55.

